Water Resources Variability in Africa during the XXth Century (Proceedings of the Abidjan'98 Conference held at Abidjan, Côte d'Ivoire, November 1998). IAHS Publ. no. 252, 1998.

Modes of climatic variability in the tropical Atlantic

JACQUES SERVAIN
Centre ORSTOM, BP 70, F-29280 Plouzané, France
e-mail: servain@orstom.fr

ILANA WAINER
Dept. Oceanográfia Fisíca, Universidade de São Paulo, Praça do Oceanográfico, 19105508-900 São Paulo, Brazil

ALAIN DESSIER
Centre ORSTOM de Brest, BP 70, F-29270 Plouzané, France

JULIAN P. McCREARY, Jr
Oceanographic Center, Nova Southeastern University, 8000 N. Ocean Drive, Dania, Florida 33004, USA

Abstract The tropical Atlantic Ocean exhibits two primary modes of interannual climate variability: an "equatorial mode" analogous to, but weaker than, the Pacific El Niño phenomenon, and a "dipole" mode that does not have a Pacific counterpart. The equatorial mode is responsible for warm (and cold) sea surface temperature (SST) events in the Gulf of Guinea, and is identifiable with changes in the equatorial thermocline slope resulting from zonal-wind anomalies in the western tropical Atlantic. The dipole mode is characterised by SST anomalies of opposite sign on either side of the mean position of the Intertropical Convergence Zone (ITCZ). To date, the dipole mode has been detected in the ocean only from SST. Here it is shown, using surface and subsurface oceanic temperatures obtained from observations as well as from a numerical solution, that the dipole mode is linked to changes in the equatorial thermocline slope occurring at interannual time scales. Thus, the two main interannual climatic modes appear to be dynamically linked in this frequency band. Furthermore, the dominant pattern of variability in both modes involves north–south displacements of the ITCZ, as in the annual response.

INTRODUCTION

During the last decade, a number of studies have identified two primary modes of interannual climate variability in the tropical Atlantic (e.g. Servain & Merle, 1993). One of them, the "equatorial" mode, has a time scale of 2–4 years. It is similar to, albeit much weaker than, the Pacific El Niño-Southern Oscillation (ENSO) in that it relates changes in the tropical ocean's thermal structure to trade-wind anomalies in the western equatorial ocean. Specifically, when the trades intensify (weaken) in the western Atlantic, the equatorial thermocline slope increases (decreases), and negative (positive) SST anomalies develop in the eastern equatorial ocean, particularly in the Gulf of Guinea (Servain & Arnault, 1995). The second mode, the "dipole" mode,

has no Pacific counterpart. It is characterized by a north–south interhemispheric gradient of SST anomalies, and its time scale ranges from interannual to decadal (Moura & Shukla, 1981; Servain, 1991). During typical dipole episodes, anomalies appear with opposite signs on either side of the Intertropical Convergence Zone (ITCZ), although the development is not always simultaneous (Houghton & Tourre, 1992). So far, this mode has been observed mainly in SST and surface wind fields, and little is known about its subsurface manifestations.

Here, we use both observed and simulated, oceanic temperature data to address the question of whether the two modes interact with each other. First, we describe the data sets used in our analyses and then review the basic properties of the modes, among other things describing their identifying characteristics. Then, we define quantitative measures of these characteristics, and compare their time series for the period 1985–1994. Based on the good correlation between the measures, we find that both modes involve fluctuations of the equatorial thermocline slope on the same time scale (2–4 year period). Furthermore, they are associated with anomalous north–south shifts in the location of the ITCZ, similar to what happens in the seasonal cycle. Our results therefore suggest that the two modes are linked to each other at interannual time scales, and that both can be viewed as being modifications of the normal annual cycle.

DATA SOURCES

Owing to the increasing amount of surface marine observations obtained from the Volunteer Observing Ship (VOS) system, SST and surface wind data are sufficient to allow a continuous temporal–spatial analysis on a $2° \times 2°$ grid over the tropical Atlantic at least since 1964. The 1985–1993 SST and wind observations used here are obtained from the monthly analysis of Servain *et al.* (1985, 1996).

In contrast to the surface data, it is difficult to obtain a continuous basinwide picture of the observed oceanic properties below the ocean's surface. Historical subsurface data are obtained mainly from expendable bathythermograph (XBT) drops. As for the surface data set, these observations are available from the VOS system, but in far fewer numbers, and their coverage is restricted to the primary ship tracks. In the tropical Atlantic, two ship tracks, AX11 (Europe–South America) and AX15 (Europe–South Africa) shown in Fig. 1, are sampled densely enough to allow continuous monthly coverage, and then only since the beginning of the Tropical Ocean and Global Atmosphere (TOGA) program in the mid-1980s when intensive subsurface observations first began to be taken (Fabri *et al.*, 1996).

To corroborate and expand upon the rather sparse, subsurface observations, we also utilize a solution from OPA-7, an ocean general circulation model (OGCM) developed at the Laboratoire d'Océanologie et de Dynamique du Climat (Delécluse *et al.*, 1993). In the specific solution used here, OPA-7 is forced by wind-stress, heat-flux, and precipitation fields provided by ARPEGE, an atmospheric general circulation model (AGCM) developed at Météo-France (Déqué *et al.*, 1994). The AGCM was run during the TOGA period (1985–1994) using observed SST (Reynolds & Smith, 1994).

The oceanic model covers the Atlantic from 50°N to 50°S, but is entirely prognostic only between 20°N and 20°S. Poleward of these latitudes, the solution is

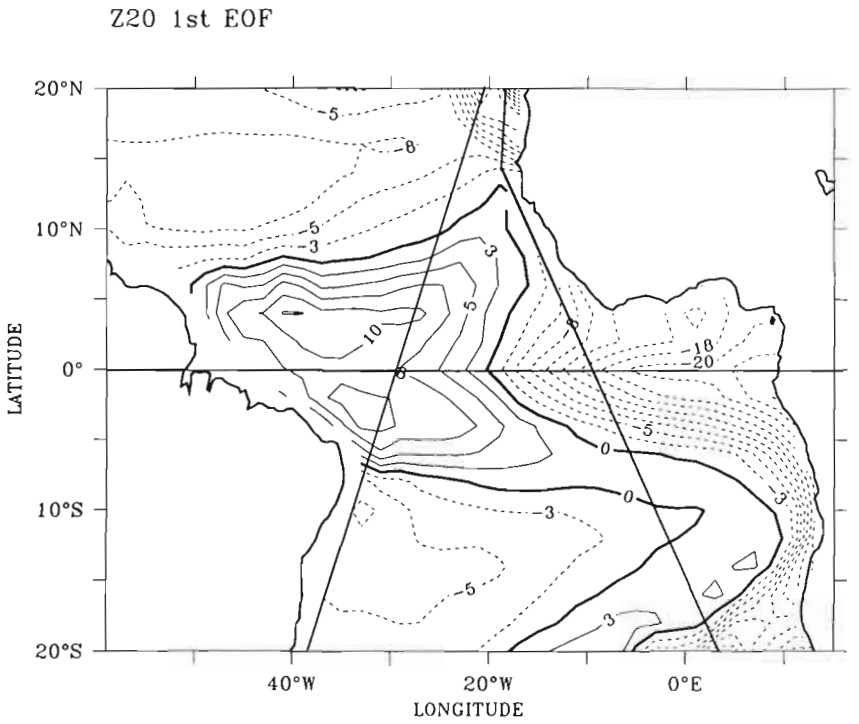

Fig. 1 Spatial structure of the first EOF of Z20 monthly anomalies from the numerical solution. Straight lines indicate ship tracks AX11 (west) and AX15 (east).

slowly restored towards Levitus (1982) climatology below the mixed layer. In addition, the model's resolution varies with latitude, from $\Delta y = 0.33°$ near the equator to $\Delta y = 1.50°$ in the subtropics. These properties suggest that OPA-7 is able to simulate climatic variability more realistically near the equator than elsewhere.

OVERVIEW

Equatorial mode

Figure 1 illustrates the tropical-ocean thermal structure during the "cold phase" of the equatorial mode in the numerical solution noted above. It shows the depth anomaly of the 20°C isotherm (hereafter referred to as Z20), which is a typical temperature for the mid-thermocline in the tropics. In fact, Fig. 1 is really the spatial pattern of the first mode of an empirical orthogonal function (EOF) analysis performed on the Z20 anomaly field, and it explains 84% of the variance. Similar, but less complete, patterns are derivable from observed Z20 fields (e.g. Reverdin *et al.*, 1991).

It is well known that ocean dynamics play a prominent role in the generation of Z20 anomaly patterns like those in Fig. 1, and in the development of interannual SST anomalies in the eastern equatorial ocean; hence, they are important in the equatorial mode itself. Consider the response to strengthened trade winds in the western ocean. They excite equatorially trapped, Kelvin waves that propagate eastward across the

basin in a few weeks time, shallow the thermocline in the eastern, equatorial ocean, and increase the equatorial tilt of Z20. They subsequently reflect from the eastern boundary as Rossby waves and coastal Kelvin waves, thereby extending the response throughout the eastern ocean and to latitudes well off the equator. Because the thermocline shallows throughout the eastern ocean, cool subsurface water is able to upwell to the surface more readily, thereby creating cool SST anomalies in the region. The pattern in Fig. 1 results from such processes, and its opposite occurs in response to weakened trades. Observational evidence for this type of dynamic response can be found in Moore *et al.* (1978), Picaut (1983), and Katz (1987, 1997). More detailed discussions of the relevant theory can be found in Philander (1979), McCreary *et al.* (1984), Zebiak (1993) and Servain & Arnault (1995).

A well-documented warm phase of the equatorial mode took place in 1984, when equatorial monthly anomalies of SST reached 3–4°C near the African coast and the equatorial thermocline slope became unusually flat (Philander, 1986; Servain & Séva, 1987; Reverdin *et al.*, 1991). Other warm episodes took place in 1968, 1995 and 1997, whereas significant cold events were noted in 1967 and 1976. Such events have important climatic, social, and economical consequences. The African monsoon feels their impact in that the distribution and intensity of precipitation is strongly affected. For example, during 1968 there were strong rains along several African countries bordering the Gulf of Guinea (Hisard, 1980), while sub-Saharan Africa (Sahel) was very dry (Lamb, 1978b). In addition, these events affect open-ocean tuna fishing (Fonteneau, 1991), as well as the distribution of several pelagic species along the African coast (Binet, 1982; Binet & Marchal, 1993).

Dipole mode

At the surface, the observed dipole mode is associated with spatially coherent SST and wind patterns of opposite sign on either side of the mean position of ITCZ (Moura & Shukla, 1981; Servain, 1991; Nobre & Shukla, 1996). It is also associated with slow interannual shifts in the mean position of the ITCZ, and can be seen across a broad range of time scales from seasonal to decadal (Servain, 1991; Mehta & Delworth, 1995).

To illustrate the dipole mode, Fig. 2 plots the first EOF of SST for the numerical solution. In this case, the variance accounted for is 45%. Consistent with patterns determined from observations (e.g. Moura & Shukla, 1981, or Nobre & Shukla, 1996), the anomaly pattern in Fig. 2 exhibits a dipole structure with opposite SST anomalies on either side of the mean position of the ITCZ, which is the defining criterion for the dipole mode. In contrast to the observed structure, however, it does not show distinct centres of action confined in the subtropics. The likely cause of this discrepancy is the property that OPA is relaxed toward climatological SST poleward of 20°, and hence cannot maintain SST anomalies there.

In contrast to the equatorial mode, the ocean dynamics associated with the dipole mode are not well understood. Indeed, recent studies suggest that it has a purely thermodynamic origin (Carton *et al.*, 1996; Chang *et al.*, 1997). Nevertheless, even if ocean thermodynamics is instrumental in determining the origin of the interhemispheric SST anomalies, dynamic processes probably still play some role. In the Chang *et al.* (1997) coupled model, for example, although positive feedback is

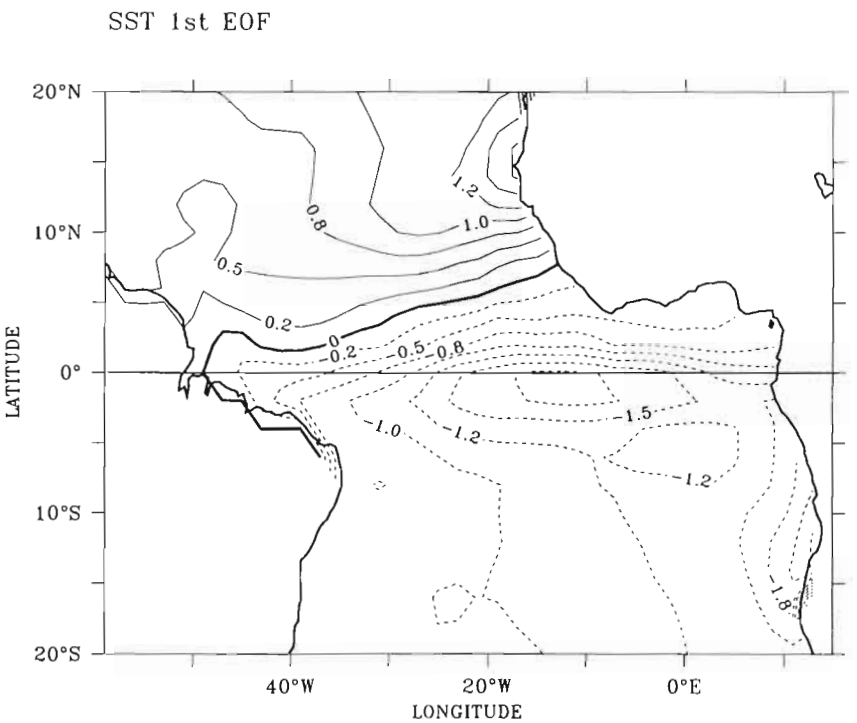

Fig. 2 Spatial structure of the first EOF of SST monthly anomalies from the numerical solution.

generated thermodynamically by a mutual interaction between the wind-induced heat flux and SST, ocean dynamics (temperature advection) provides the negative feedback that sets the long time scale of the variability.

The dipole mode is best known for its effect on droughts in Northeast Brazil (Nordeste). Periods of increased (decreased) rainfall there are generally associated with an anomalous displacement of the ITCZ towards the south (north), and also with a pattern of anomalous cold (warm) SST in the northern tropical Atlantic and warm (cold) SST in the southern tropical Atlantic (Servain, 1991; Wainer & Soares, 1997). For instance, such anomalous patterns occurred during early 1974 and 1985, the last two major wet periods in Nordeste (Servain *et al.*, 1998). Likewise, droughts in Sahel (like the major one in 1968) are often found to be associated with a broad band of negative (positive) SST anomalies across the tropical North (South) Atlantic (Lamb, 1978a).

RESULTS

Observations

As noted above, the equatorial mode is characterized by changes in the slope of the equatorial thermocline, and the dipole mode is characterized by interhemispheric SST anomalies with opposite signs on either side of the ITCZ. To estimate the equatorial

thermocline slope from observations, we utilized the 1985–1993 XBT data along the AX11 and AX15 tracks (Fig. 1) filtered to remove the climatological annual cycle. These time series give Z20 at two locations on the equator: close to 30°W for AX11 and close to 10°W for AX15. The difference between these two records is our measure of the equatorial thermocline slope, $\Delta Z20$. Positive (negative) values of $\Delta Z20$ correspond to a rather pronounced (rather flat) thermocline slope. To measure the interhemispheric SST gradient, ΔSST, we used the difference between anomalous SST averaged from 5°–20°N and from 5°–15°S, a method similar to that utilized previously by Servain (1991) for his Atlantic-dipole index. Positive (negative) values of ΔSST correspond to a SST dipole pattern that is warm (cold) in the northern ocean and cold (warm) in the equatorial and southern regions.

Finally, based on the observed wind data set, we determined a monthly index of the anomalous latitudinal position of the ITCZ, $\Delta ITCZ$, for the period 1985–1993. It is defined to be the abnormal latitudinal displacement of the zero value of the meridional wind along 28°W, a meridian near the centre of the basin. Positive (negative) values of $\Delta ITCZ$ identify a northward (southward) abnormal position of ITCZ.

All three (6-month smoothed) indices ($\Delta Z20$, ΔSST and $\Delta ITCZ$) are plotted in Fig. 3. Three main 2–3 year oscillations, in which the SST dipole evolves from a negative to a positive state and returns, can be seen during the study period: 1986–1989, 1989–1991 and 1991–1993. At the same time, the tilt of Z20 along the equator evolves similarly, from negative conditions (a flat thermocline) to positive conditions (a pronounced slope) and returns. It is visually apparent that ΔSST and $\Delta Z20$ are well

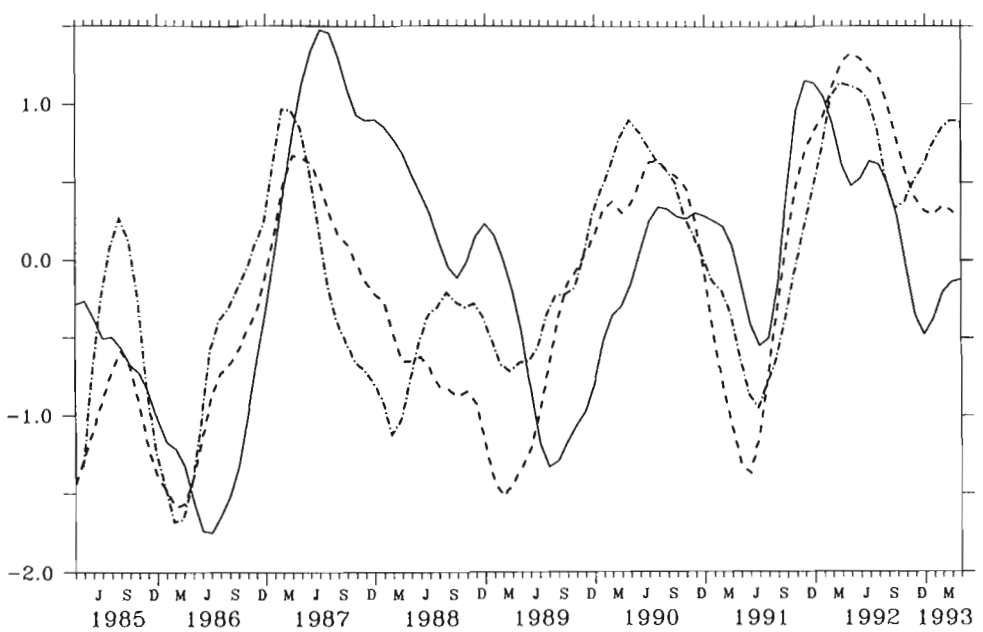

Fig. 3 Time series of ΔZ20 (solid curve), ΔSST (dashed curve), and ΔITCZ (dashed/dotted curve) from the observations. The time series are all smoothed by a 6-month running-mean filter. For a better readability, the ΔZ20 curve is forwarded by 2 months *vs* the two other series.

correlated on a 2–4 year time scale, and the maximum correlation coefficient between them is 0.65 with a 2-month lag (ΔSST leading). This good correlation suggests that the equatorial and dipole modes, the primary modes of interannual variability in the tropical Atlantic, are significantly linked at interannual time scale.

As expected, the correlation coefficient between $\Delta ITCZ$ and ΔSST is high (maximum correlation of 0.83 at zero lag), a northward (southward) deviation of ITCZ corresponding to positive (negative) SST dipole pattern. The correlation between $\Delta ITCZ$ and $\Delta Z20$ is somewhat weaker (a maximum coefficient 0.45 at 2-month lag, $\Delta ITCZ$ leading), although it is visually evident that the two time series have a similar temporal evolution.

Model

The spatial patterns of the solution's equatorial and dipole modes are well characterized by the first EOFs of the Z20 and SST anomaly fields (Figs 1 and 2, respectively). Figure 4 shows the time series of each EOF, smoothed with a 6-month running-mean filter. It is visually apparent that the two time series are quite similar on a 2–4 year time scale. Indeed, the maximum correlation is 0.73 with a 1-month lag, Z20 leading. This similarity shows that the two interannual modes are as closely related in the numerical solution as they are in the observations. To compare the solution more closely to the observations, Fig. 5 shows curves for the solution that exactly correspond to curves $\Delta Z20$ and ΔSST in Fig. 3. The two curves are similar

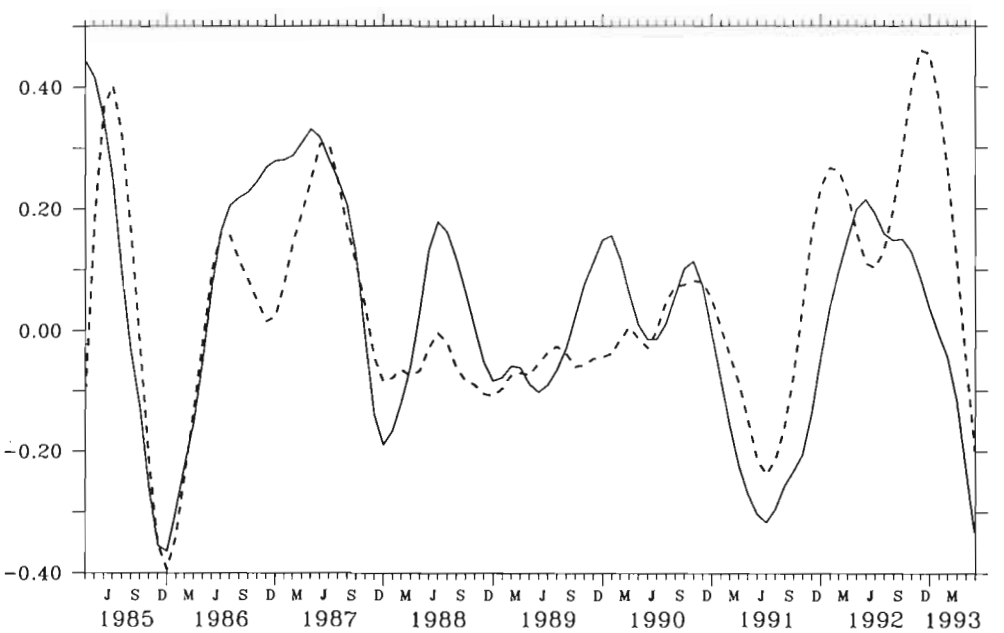

Fig. 4 Time series associated with the first EOFs of the Z20 anomalies (solid curve) and SST (dashed curve) monthly anomalies from the numerical solution, both smoothed by a 6-month running-mean filter.

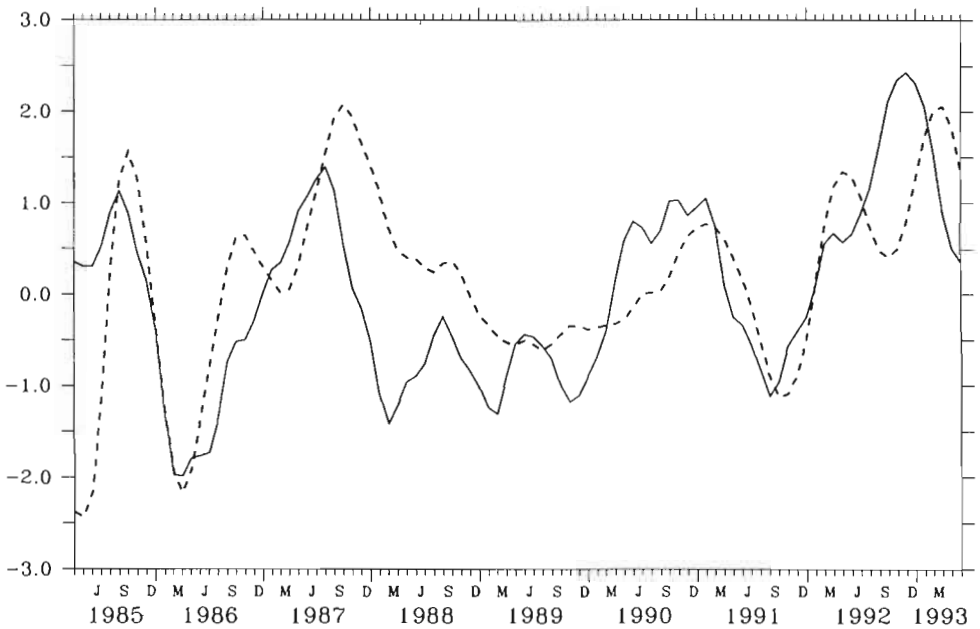

Fig. 5 Time series ΔZ20 (solid curve) and ΔSST (dashed curve) from the numerical solution, both smoothed by a 6-month, running-mean filter.

both to each other (with a maximum correlation of 0.61 at 1-month lag, Z20 leading) and to the observed set (Fig. 3). This supports, *a posteriori*, that the interannual signal provided by the numerical solution is reasonably consistent with the observations, and thus can be used to illustrate the main modes of interannual variability of the tropical Atlantic, as described above.

CONCLUDING REMARKS

For the first time, it is shown that the equatorial mode and the dipole mode, the two main modes of climatic variability in the tropical Atlantic, are linked at interannual time scales. Moreover, the processes involved seem to be of the same nature as those that control the seasonal cycle. A possible scenario for the "cold" phase of an oscillation is as follows: An anomalous northward displacement of the ITCZ ($\Delta ITCZ > 0$) weakens the northeast trades, and strengthens the southeast trades and equatorial zonal winds; these changes increase the equatorial thermocline tilt ($\Delta Z20 > 0$), warm SST north of the ITCZ due to a decrease in evaporative cooling, and cool it in the eastern-equatorial and southern regions due to increased upwelling and latent-heat loss ($\Delta SST > 0$). This situation favours drought in the Nordeste region and along the continental border of the Gulf of Guinea, and favours enhanced rainfall in the Sahel.

Regrettably, the paucity of the XBT observations does not allow one to obtain a time series of the observed equatorial thermocline tilt longer than the 1985–1993 record discussed here. Due to its shortness (9 years), it is not possible to conclude

that such processes link the two modes at decadal time scales. Given their strong connection at interannual time scales, however, this possibility seems likely. We are currently working to demonstrate this linkage, and to obtain a better understanding of the dynamic and thermodynamic processes that govern the two modes at all frequencies.

Acknowledgements The XBT data were collected, validated and archived at the TOGA-WOCE Centre in Brest, France. The numerical simulation was performed at the "Laboratoire d'Océanologie Dynamique et de Climatologie" (LODYC/UMR 121) of l'Université de Paris 6, France, and results were made available to us by Claire Levy. We would like to thank Pascale Delécluse for comments and helpful discussions during this research. This work was supported in part by COFECUB agreement no. 27/96-97 between the ORSTOM Centre at Brest, France and the Oceanography Institute of the University of São Paulo, Brazil, and by NOAA Grant NA76GP0353 through the GOALS programme.

REFERENCES

Binet, D. (1982) Influence des variations climatiques sur la pêcherie des Sardinella aurita ivoiro-ghanéenne: relation sécheresse-surpêche. *Oceanologica Acta* **5**, 443–452.

Binet, D. & Marchal, E. (1993) The large marine ecosystem of shelf areas in the Gulf of Guinea: long-term variability induced by climatic changes. In: *Large Marine Ecosystems: Stress, Mitigation and Sustainability* (ed. by K. Sherman, L. W. Alexander & B. D. Gold), 104–118. AAAS Press, USA.

Carton, J. A., Cao, X., Giese, B. S. & da Silva, A. M. (1996) Decadal and interannual SST variability in the tropical Atlantic. *J. Phys. Oceanogr.* **26**, 1165–1175.

Chang, P., Ji, L. & Li, H. (1997) A decadal climate variation in the tropical Atlantic Ocean from thermodynamic air–sea interactions. *Nature* **385**, 516–518.

Delécluse, P., Madec, G., Imbard, M. & Levy, C. (1993) OPA version 7 ocean general circulation model reference manual. Rapport Interne LODYC 93/05. LODYC, Université Paris VI, Paris, France.

Déqué, M., Dreveton, C., Braun, A. & Cariolle, D. (1994) The ARPEGE/IFS atmosphere model: a contribution to the French community climate modelling. *Clim. Dyn.* **10**, 248–266.

Fabri, M. C., Dessier, A., Maudire, G., Raguenes, Y. & Rebert, J.-P. (1996) Global subsurface data Centre (GSDC) for TOGA and WOCE. *International WOCE Newslett.* **22**, 18–20.

Fonteneau, A. (1991) Les anomalies de l'environnement en 1984 dans le Golfe de Guinée. Effets possibles sur la capturabilté de l'albacore. *Rec. Doc. Scient. ICCAT* **36**, 380–408.

Hisard, P. (1980) Observation de réponses de type "El Nino" dans l'Atlantique tropical, Golfe de Guinée. *Oceanologica Acta* **3**, 69–78.

Houghton, R. W. & Tourre, Y. (1992) Characteristics of low-frequency sea surface temperature fluctuations in the tropical Atlantic. *J. Climate* **5**, 765–771.

Katz, E. J. (1987) Equatorial Kelvin waves in the Atlantic. *J. Geophys. Res.* **92**, 1894–1898.

Katz, E. J. (1997) Waves along the equator in the Atlantic. *J. Phys. Oceanogr.* **27**, 2536–2544.

Lamb, P. J. (1978a) Large-scale tropical Atlantic surface circulation anomalies associated with sub-saharan weather anomalies. *Tellus* **30**, 240–251.

Lamb, P. J. (1978b) Case studies of tropical Atlantic surface circulation pattern during recent sub-saharan weather anomalies: 1967 and 1968. *Mon. Weath. Rev.* **106**, 482–491.

Levitus, S. (1982) Climatological atlas of the World Ocean. NOAA Prof. Pap. 13, US Government Printing Office, Washington DC, USA.

McCreary, J. P., Picaut, J. & Moore, D. W. (1984) Effects of remote annual forcing in the eastern tropical Atlantic Ocean. *J. Mar. Res.* **42**, 45–81.

Mehta, V. M. & Delworth, T. (1995) Decadal variability of the tropical Atlantic Ocean surface temperature in shipboard measurements and in a global ocean–atmosphere model. *J. Climate* **8**, 172–190.

Moore, D. W., Hisard, P., McCreary, J., Merle, J., O'Brien, J., Picaut, J., Verstraete, J. M. & Wunsch, C. (1978) Equatorial adjustment in the eastern Atlantic. *Geophys. Res. Lett.* **5**, 637–640.

Moura, A. D. & Shukla, J. (1981) On the dynamics of droughts in northeast Brazil: observations, theory and numerical experiments with a general circulation model. *J. Atmos. Sci.* **38**, 2653–2675.

Nobre, P. & Shukla, J. (1996) Variations of sea surface temperature, wind stress, and rainfall over the tropical Atlantic and South America. *J. Climate* **9**, 2464–2579.

Philander, S. G. H. (1979) Variability of the tropical oceans. *Dyn. Atmos. Ocean* **3**, 191–208.

Philander, S. G. H. (1986) Unusual conditions in the tropical Atlantic Ocean in 1984. *Nature* **322**, 236–238.

Picaut, J. (1983) Propagation of the seasonal upwelling in the eastern equatorial Atlantic. *J. Phys. Oceanogr.* **13**, 18–37.

Reverdin, G., Delécluse, P., Lévy, C., Andrich, P., Morlière, A. & Verstraete, J. M. (1991) The near surface tropical Atlantic in 1982–1984: Results from a numerical simulation and a data analysis. *Prog. Oceanogr.* **27**, 273–340.

Reynolds, R. W. & Smith, T. M. (1994) Improved global sea surface temperature analyses using optimum interpolation. *J. Climate* 7, 929–948.

Servain, J. (1991) Simple climatic indices for the tropical Atlantic Ocean and some applications. *J. Geophys. Res.* **96**, 15.137–15.146.

Servain, J. & Arnault, S. (1995) On forecasting abnormal climatic events in the tropical Atlantic Ocean. *Ann. Geophys.* **13**, 995–1008.

Servain, J. & Merle, J. (1993) Interannual climate variations over the tropical Atlantic Ocean. In: *Prediction of Interannual Climate Variations* (ed. by J. Shukla), 153–171. NATO ASI

Series, vol. 16, Springer-Verlag, Berlin, Germany.

Servain, J. & Séva, M. (1987) On relationships between tropical Atlantic sea surface temperature, wind stress and regional precipitation indices: 1964–1984. *Ocean-Air Interactions* **1**, 183–190.

Servain, J., Picaut, J. & Busalacchi, A. J. (1985) Interannual and seasonal variability of the tropical Atlantic Ocean depicted by sixteen years of sea surface temperature and wind stress. In: *Coupled Ocean-Atmosphere Models* (ed. by J. C. J. Nihoul), 211–237. Elsevier Science Publishers, Amsterdam, The Netherlands.

Servain, J., Stricherz, J. N. & Legler, D. M. (1996) *TOGA Pseudo-stress Atlas 1985–1994*—vol. 1: *Tropical Atlantic*. Centre ORSTOM de Brest, France.

Servain, J., Busalacchi, A. J., McPhaden, M. J., Moura, A. D., Reverdin, G., Vianna, M. & Zebiak, S. E. (1998) A Pilot Research moored Array in the Tropical Atlantic (PIRATA). Accepted in *Bull. Am. Met. Soc.*

Wainer, I. & Soares, J. (1997) North Northeast Brazil rainfall and its decadal—scale relationship to wind stress and sea surface temperature. *Geophys. Res. Lett.* **24**, 277–280.

Zebiak, S. E. (1993) Air–sea interaction in the equatorial Atlantic region. *J. Climate* **6**, 1567–1586.